



**HAL**  
open science

# Estimation of rare event probabilities in power transmission networks subject to cascading failures

Francesco Cadini, Gian Luca Agliardi, Enrico Zio

► **To cite this version:**

Francesco Cadini, Gian Luca Agliardi, Enrico Zio. Estimation of rare event probabilities in power transmission networks subject to cascading failures. *Reliability Engineering and System Safety*, 2017, 158, pp.9-20. 10.1016/j.ress.2016.09.009 . hal-01652282

**HAL Id: hal-01652282**

**<https://hal.science/hal-01652282>**

Submitted on 30 Nov 2017

**HAL** is a multi-disciplinary open access archive for the deposit and dissemination of scientific research documents, whether they are published or not. The documents may come from teaching and research institutions in France or abroad, or from public or private research centers.

L'archive ouverte pluridisciplinaire **HAL**, est destinée au dépôt et à la diffusion de documents scientifiques de niveau recherche, publiés ou non, émanant des établissements d'enseignement et de recherche français ou étrangers, des laboratoires publics ou privés.



# Estimation of rare event probabilities in power transmission networks subject to cascading failures



Francesco Cadini<sup>a,\*</sup>, Gian Luca Agliardi<sup>a</sup>, Enrico Zio<sup>a,b</sup>

<sup>a</sup> Dipartimento di Energia – Politecnico di Milano, Via La Masa 34, I-20156 Milano, Italy

<sup>b</sup> Chair System Science and The Energy Challenge, Fondation Electricite' de France (EDF), CentraleSupélec, Université Paris-Saclay, Grande Voie des Vignes, 92290 Chatenay-Malabry, France

## ARTICLE INFO

### Keywords:

Power transmission networks  
Cascading failures  
Rare event probabilities  
Monte Carlo  
Kriging  
Latin Hypercube

## ABSTRACT

Cascading failures seriously threaten the reliability/availability of power transmission networks. In fact, although rare, their consequences may be catastrophic, including large-scale blackouts affecting the economics and the social safety of entire regions. In this context, the quantification of the probability of occurrence of these events, as a consequence of the operating and environmental uncertain conditions, represents a fundamental task. To this aim, the classical simulation-based Monte Carlo (MC) approaches may be impractical, due to the fact that (i) power networks typically have very large reliabilities, so that cascading failures are rare events and (ii) very large computational expenses are required for the resolution of the cascading failure dynamics of real grids. In this work we originally propose to resort to two MC variance reduction techniques based on metamodeling for a fast approximation of the probability of occurrence of cascading failures leading to power losses. A new algorithm for properly initializing the variance reduction methods is also proposed, which is based on a smart Latin Hypercube search of the events of interest in the space of the uncertain inputs. The combined methods are demonstrated with reference to the realistic case study of a modified RTS 96 power transmission network of literature.

## 1. Introduction

In recent years, power outages and interruptions have been occurring in many countries, with large consequences. For example, the major of Northeast America in 2003 caused a 6 billion dollars economic loss for the region [1,2] and several other social consequences of power interruptions, e.g. related to transportation, food storage and credit card operations, just to mention a few of them [3].

Blackouts are the outcomes of cascades of failures, initiated, in turn, by the failures of a limited set of components, due, for example, to overloads generated by excessive load demands, loss of generation, human errors in network operation, or to external events, e.g. caused by extreme environmental conditions, such as lightning, icing, floods, wind storms, earthquakes, etc. Subsequently, other components fail and are disconnected to avoid further severe damage.

Traditionally, a power transmission network is designed and operated so that a single component disconnection cannot give rise to cascading failures ( $N - 1$  criterion [4]); however, rare combinations of circumstances, uncommon events or inadequate countermeasures may result in further line disconnections, eventually leading to failure propagation. Extremely severe natural events may even directly fail the

components of the network.

In this work, we propose to evaluate the reliability of a power transmission network operating under uncertain environmental conditions. Quantitatively, the problem amounts to computing the probability that an initial, limited outage yields a cascading failure with final load shedding larger than zero (or any other predefined threshold).

Mathematically, the problem can be framed as follows. We consider the model  $\mathcal{G}$  of the system response  $Y$  to the vector of uncertain inputs  $\mathbf{x}$ :

$$Y = \mathcal{G}(\mathbf{x}) \quad (1)$$

where  $\mathbf{x}$  is a  $n$ -dimensional random vector  $\mathbf{x} = \{x_1, x_2, \dots, x_n\}$ , with probability density function (pdf)  $f(\mathbf{x})$ . The model  $\mathcal{G}(\mathbf{x})$  is often called the system performance function. The system failure is usually defined as the event  $\{\mathcal{G}(\mathbf{x}) > 0\}$ , where the set of values  $\mathbf{x} : \mathcal{G}(\mathbf{x}) = 0$  is defined as limit state and  $\mathbf{x} : \mathcal{G}(\mathbf{x}) > 0$  is called failure domain. Then, the system failure probability is:

$$P_f = P[\mathcal{G}(\mathbf{x}) > 0] \quad (2)$$

In the present work, the performance function  $\mathcal{G}(\mathbf{x})$  is given by the combination of the network line failure model and the cascading failure

\* Corresponding author.

E-mail address: [francesco.cadini@polimi.it](mailto:francesco.cadini@polimi.it) (F. Cadini).

model, whose output is the final load shedding, as it will further detailed in Section 4. Correspondingly, the failure probability  $P_f$  is the probability that an outage yields a cascading failure event leading to a final load shedding larger than zero.

Simulation-based methods, i.e. Monte Carlo (MC) computational schemes, are the most widely used for estimating the probability of failure  $P_f$ . In the crude MC scheme, a large number ( $N_{MC}$ ) of input vector values  $\mathbf{x}$  is sampled from the joint pdf  $f(\mathbf{x})$  and the performance function  $\mathcal{G}(\mathbf{x})$  is evaluated in correspondence of the available  $N_{MC}$  input points. A failure indicator variable is defined as:

$$I_F(x_i) = \begin{cases} 1 & \text{if } \mathcal{G}(x_i) > 0 \\ 0 & \text{if } \mathcal{G}(x_i) \leq 0 \end{cases} \quad (3)$$

The sample mean of the values of the indicator variable obtained is the MC-based estimator of the failure probability:

$$P_f \approx \hat{P}_f = \frac{1}{N_{MC}} \sum_{i=1}^{N_{MC}} I_F(x_i) \quad (4)$$

The accuracy of the estimates can be expressed in terms of the coefficient of variation ( $\delta$ ), defined as the ratio of the sample standard deviation and  $\hat{P}_f$  [1]:

$$\hat{\delta}_{MC} = \sqrt{\frac{1 - \hat{P}_f}{\hat{P}_f N_{MC}}} \quad (5)$$

Two difficulties may arise: on one hand, power networks have very large reliabilities and cascading failures are rare events; on the other hand, the computational expenses needed for the resolution of the complex models of power flows within the network become soon prohibitive, as the accuracy and level of realistic details to be included in the analysis increase.

For a computationally expensive performance function  $\mathcal{G}(\mathbf{x})$ , an accurate estimation of  $P_f$  becomes prohibitively time consuming when the failure probability is small. For example, if  $P_f$  is of the order of  $10^{-p}$ ,  $N_{MC}$  should be at least  $10^{p+2}$  to achieve a coefficient of variation  $\hat{\delta}_{MC}$  of the order of 10%.

In order to overcome this issue, many methods have been proposed in literature. In structural reliability analysis, for example, First or Second Order Reliability Methods (FORM or SORM) are commonly used [5–9]. These methods approximate the limit state function  $\mathcal{G}(\mathbf{x})=0$  around the so-called Most Probable Failure Point (MPFP) or “design point” by a Taylor series expansion, which allows fast analytic computations of the failure probabilities. However, these methods suffer from a major drawback, i.e. they require the numerical computation of the gradient and the Hessian of the limit state function, thus potentially leading to large and not easily quantifiable estimation errors.

Other approaches increase the efficiency of the MC estimators by resorting to so-called variance reduction techniques.

Probably, the most popular variance reduction technique is that of importance sampling (IS), which has been successfully applied in many fields of research. In IS, a suitable importance density alternative to the original input pdf  $f(\mathbf{x})$  is chosen so as to favor the MC samples to be near the failure region, thus forcing the rare failure event to occur more often. The major difficulty of the method lies in the a priori definition of a suitable importance density. In order to overcome this issue, a common approach in structural reliability is that of choosing the importance density as a joint Gaussian distribution centered around some properly identified design points [10], such as, for example, the MPFP(s) identified by a FORM (or SORM) in the isoprobabilistically transformed standard input space [9,10]: by doing so, it is possible to refine the result of the FORM (SORM) by an IS procedure, which picks the samples in the vicinity of the failure region. Another popular strategy is that of iteratively adapting the importance density by exploiting the model evaluations gathered in previous estimation steps

or, in other words, to use some adaptive pre-samples [11,12]: in order to gain this prior knowledge, usually, many performance function evaluations are required to find samples falling in the failure regions, in particular when the failure probability to be estimated is very low. To overcome this problem, [13] introduced a method based on Markov Chain Monte Carlo (MCMC), based on a modified Metropolis-Hastings algorithm (or similar schemes), to adaptively approximate the optimal importance density. In general, however, the major drawback of IS-based approaches is that for complex, high dimensional problems, it is often difficult, if not impossible, to build efficient importance densities, as observed in [14] and also demonstrated in [15].

One of the most successful variance reduction alternative technique is subset simulation (SS) [16,17], which does not suffer from this issue. The method is based on a representation of the failure probability as the product of conditional probabilities of some properly chosen “intermediate”, more frequent failure events, the estimation of each of which only requires few performance function evaluations. The conditional probabilities are, then, sampled by means of a MCMC method. However, the total number of evaluations required remains too large in many applications requiring long-running computer codes [18], so that the failure probability estimation may still be computationally prohibitive. Moreover, the method's efficiency stems from i) a smart definition of the “intermediate” failure events, which is not an easy task, especially for complex models with little or no availability of prior information, and ii) the crucial choice of the proposal pdfs, which is, in general, significantly dependent on the problem under analysis, thus limiting somewhat the flexibility of the approach [16].

Another important class of variance reduction methods successfully addressing the problem of large dimensionality is that based on line sampling (LS) [19], which uses lines, instead of points, to probe the failure domain. The method stems from the determination of an important direction pointing towards the failure domain, with respect to which the sampling lines are then defined, thus giving rise to conditional, one-dimensional problems, simpler to solve. However, similarly to SS, the method still requires too many performance function evaluations in many applications. Moreover, the efficient determination of the principal direction is still an open issue, which significantly depends on the application under analysis [19].

Recently, effective strategies for further reducing the computational efforts required by small failure probability estimation have been proposed, which use a surrogate model (metamodel) for a fast approximation of the performance function within a sampling based Monte Carlo scheme. To run a metamodel is, in fact, orders of magnitude faster than the original model, thus potentially allowing significant computational savings. In this context, the Adaptive Kriging MC Sampling (AKMCS) algorithm [20] and its improved version Adaptive Kriging Importance Sampling (AKIS) [21,22] have been recently proposed, where a Kriging-based metamodel is coupled to a MC-based strategy (crude, in AKMCS, and IS, in AKIS), within an adaptive learning scheme which automatically refines the metamodel to a desired level of precision. These methods have been demonstrated efficient in estimating small failure probabilities in different engineering fields, from structural reliability [20–22] to probabilistic risk analysis of nuclear installations [23–26]. However, the most attractive feature of this class of methods, which stimulated their application in this work, is the fact that they require very little calibration when applied to different problems, demonstrating high levels of adaptability and flexibility, as opposed to most of the methods illustrated above. A further motivation for the use of Kriging in the present context lies in the successful demonstration of its applicability for approximating step-wise discontinuous functions given by [24], provided that proper care is taken in the construction of the metamodel DoE.

Thus, in the present work, we propose to exploit this feature for the analysis of the reliability of power networks subject to cascading failures, a context very different from that of structural reliability, for which these methods were first introduced. Yet, in order to be able to

exploit the algorithm flexibility, a new initialization algorithm is needed to account for the specific peculiarities of these systems and of their performance function  $\mathcal{G}(x)$ : when a cascading failure is successfully controlled (which should be the case in most of the line failure events), the final load shedding is always equal to zero, i.e.,  $\mathcal{G}(x)=0$ . This means that the initial small set of performance functions evaluations needed by the AKMCS (AKIS) in order to build the first Kriging-based metamodel, which would then be progressively refined by the adaptive module of the algorithm (see Section 2), would most likely contain only examples with output (i.e. the load shedding) equal to zero. Thus, if in correspondence of several inputs the related outputs are always equal to the same constant value (zero), the meta-model cannot learn the behavior of the performance function in correspondence of input points leading to a load shedding larger than zero, and the AKMCS (AKIS) does not work.

However, a single point of failure in the input space is sufficient for properly initializing the adaptive scheme for the refinement of the Kriging-based metamodel, and we develop a new computational strategy based on a Latin-Hypercube search of the input space in order to identify it [27]. The proposed modification, called Latin Hypercube-based Sampling Algorithm (LHSA), is, then, coupled to the AKMCS (AKIS). The resulting estimation tool is demonstrated on the realistic case study of the RTS 96 power transmission network of literature [28], modified in [29,30] to account for the contribution of two wind farms connected to the grid, where cascading failures are realistically simulated resorting to a direct current (DC) approximation of the power flowing in the network lines.

The rest of the paper is structured as follows. Section 2 describes the procedure and methodology of the analyzed models: first the AKMCS and AKIS simulation techniques are recalled in Section 2.1, and, then, insights on the LHSA sampling scheme are given in Section 2.2. In Section 3.1 and Section 3.2, the proposed algorithm is validated on a simple case study and on an analytical case taken from literature, respectively. The test networks specification, the cascade model, the restoration strategy as well as the Sequential Monte Carlo procedure are presented in Section 4. In Section 5 conclusions are given.

## 2. Failure probability estimation algorithm

### 2.1. The Adaptive-Kriging Monte Carlo Sampling and importance sampling methods (AKMCS and AKIS)

In this work, we propose to resort to the efficient Adaptive Kriging Monte Carlo Sampling (AKMCS) technique introduced in [20] and its improved version, the Adaptive Kriging Importance Sampling (AKIS) [21]. In what follows, we briefly recall the basic idea underlying the functioning of the algorithms; for further details, the interested reader may refer to [20] and [21].

The AKMCS exploits the idea of replacing a computationally expensive  $\mathcal{G}(x)$  with a fast-to-evaluate Kriging-based surrogate model, built on the basis of a set of  $N$  available evaluations of  $\mathcal{G}(x)$  performed in correspondence of properly selected inputs, within an adaptive Monte Carlo scheme which allows to gradually improve the surrogate model precision, while performing the failure probability estimation.

The Kriging approximation considers the performance function  $\mathcal{G}(x)$  as a realization of a Gaussian process with mean  $\mu_{\hat{G}}(x)$  and variance  $\sigma_{\hat{G}}^2(x)$  [31], whose parameters are identified by an optimization procedure based on a set of  $N$  available examples, also called the Design of Experiment (DoE) [32].

A population of  $N_{AKMCS}$  points  $x_i$ ,  $i=1, \dots, N_{AKMCS}$ , is sampled from  $f(x)$  and labeled as failure and safe points by the Kriging-based metamodel. An estimate of the failure probability can, then, be obtained as

$$\hat{P}_{f,AKMCS} = \frac{1}{N_{AKMCS}} \sum_{i=1}^{N_{AKMCS}} \hat{I}_f(x_i) \quad (6)$$

where  $\hat{I}_f(x_i)$  is the value of the indicator function obtained by substituting the Kriging-based approximation  $\mu_{\hat{G}}(x_i)$  to  $\mathcal{G}(x_i)$  in (3).

The estimate of the failure probability  $\hat{P}_{f,AKMCS}$  is iteratively updated. At each iteration, an active learning function [33] is used to identify the best new sample among the  $N_{AKMCS}$  available ones to be added to the DoE in order to maximize the metamodel improvement. In order to do so, the original performance function  $\mathcal{G}$  is evaluated in correspondence of the input point characterized by the most uncertain classification and added to the DoE, so as for the metamodel to become more accurate and precise in proximity of the boundary between failure and safe input points [20–22,33]. For reasons which will be shortly explained, the iterations are organized in successive batches of size  $M_m$ , labeled by an index  $m = 0, 1, 2, \dots$ . The first batch groups the first  $M_0$  iterations ( $M = 200$  for  $m = 0$ ). Operatively, the procedure proceeds by first computing the following learning function:

$$U^{(m)}(x_i) = \frac{|\mu_{\hat{G}}(x_i)|}{\sigma_{\hat{G}}(x_i)} \quad (7)$$

at each iteration of the  $m$ -th batch, for  $i=1, \dots, N_{AKMCS}$ , where  $U^{(m)}(x_i)$  represents the normalized distance in terms of Kriging prediction standard deviations  $\sigma_{\hat{G}}(x_i)$  from the predicted limit state  $\mu_{\hat{G}}(x)=0$ . The sample  $\tilde{x}_0$  among the  $N_{AKMCS}$  available that minimizes (7) is chosen as the sample to be added to the DoE. Once the DoE is updated, a new metamodel is created and a new estimate of the failure probability can be computed again according to the steps illustrated above. In past works using the AKMCS, the iterative procedure was stopped when  $U^{(m)}(\tilde{x}_0) > U_{th}$ , with  $U_{th}=2$ , i.e. the most uncertain point in the population has a probability equal to or larger than  $\Phi(U_{th}^{(0)}=2) \approx 0.977$  of being correctly classified [33], where  $\Phi(\cdot)$  is the cdf of the standard normal distribution. In this work, we relax this stopping criterion by gradually lowering the threshold  $U_{th}^{(m)}$ , (i.e., the stopping probability  $\Phi(U_{th}^{(m)})$ ), for each successive batch  $m$  of adaptive iterations, by setting  $U_{th}^{(m+1)} = c \cdot U_{th}^{(m)}$  ( $c = 0.9$  in this work). At the same time, we halve the size of the next batch of iteration by setting  $M_{m+1} = M_m/2$ . By so doing, we facilitate the convergence of the adaptive algorithm in presence of relatively large approximation errors of the metamodel in proximity of the limit state, due to discontinuities in the first-order derivatives of  $\mathcal{G}(x)$ , or even in  $\mathcal{G}(x)$  itself, at the limit state, which is the case of the present application (as it will be shown later). In fact, even when the Kriging approximation may seem to be satisfactory, in presence of very steep transitions between the safe and the failure regions at the limit state, the Kriging predictions may still be affected by large relative errors for points very close to the limit state (see, for example, Fig. 4). Thus, as practically observed, the condition  $U^{(m)}(\tilde{x}_0) > 2$  may turn out to be too strict, so that convergence would hardly be reached. With the proposed adaptive procedure for the stopping rule, we avoid setting too low thresholds, which could compromise the metamodel performances, and we let the threshold  $U_{th}^{(m)}$  adapt to the most suitable value. We start from a relatively large size of the first batch ( $M_0=200$ ) because we want to be sure that the threshold is lowered only when further iterations of the batch would not significantly contribute to the metamodel accuracy.

The Adaptive Kriging Importance Sampling (AKIS) aims at further improving the efficiency of the AKMCS by resorting to the well know importance sampling variance reduction technique [21,22]. The AKIS relies on (i) an isoprobabilistic transformation (the Nataf transformation [34]) of the input vector  $x$  into the standard space, where the transformed uncertain inputs  $u$  are distributed according to a joint standard Gaussian distribution  $\phi_n$  and (ii) the definition of an importance density in the standard space as a joint Gaussian distribution  $\varphi_n$  centered around the estimate of the MPPF identified by means of a FORM or SORM. The diagonal elements of the corresponding covariance matrix are usually chosen to be equal to one, although different values can be used depending on the specific application,

whereas the covariances are set to zero. A population of  $N_S$  points  $\mathbf{u}_i = \{u_1, \dots, u_n\}_i$ ,  $i = 1, 2, \dots, N_S$ , is sampled from  $\varphi_n$  in the standard space. Analogously to the procedure described for the AKMCS, the input points  $\mathbf{u}_i$  are, then, classified by the Kriging-based metamodels, and the failure probability  $P_f$  can be estimated as:

$$P_f \approx \hat{P}_f = \frac{1}{N_S} \sum_{i=1}^{N_S} I_F(\mathbf{u}_i) \frac{\phi_n(\mathbf{u}_i)}{\varphi_n(\mathbf{u}_i)} \quad (8)$$

and the estimated variance of the failure probability estimator is:

$$\widehat{\text{Var}}(\hat{P}_f) = \frac{1}{N_S} \left( \frac{1}{N_S} \sum_{i=1}^{N_S} \left( I_F(\mathbf{u}_i) \frac{\phi_n(\mathbf{u}_i)}{\varphi_n(\mathbf{u}_i)} \right)^2 \right) - \hat{P}_f^2 \quad (9)$$

The importance sampling scheme coupled to FORM/SORM allows to increase the speed of convergence of the Kriging-based metamodel adaptation, by picking the new samples to add closer to the limit state, and to achieve better coefficient of variations with a smaller number of input samples  $N_S$ .

## 2.2. The Latin Hypercube-based search algorithm (LHSA)

Usually, the size of the initial DoE of the Kriging-based metamodel in both the AKMCS and the AKIS, i.e. the number of performance function evaluations required to start the adaptive algorithms, is in the order of 10–12 points randomly sampled from the original uncertainty pdfs [20–22]. Unfortunately, as anticipated in the Introduction, the particular shape of the performance function  $\mathcal{G}(\mathbf{x})$  of our problem, i.e., that is almost always equal to zero when a cascading failure is successfully controlled and larger than zero only when the cascading failures lead to load shedding, is such that the Kriging-based metamodel cannot be built, since the initial randomly sampled DoE is likely to contain only events with a constant, zero output. The problem is even worse for the AKIS, where the FORM/SORM cannot identify the MPFP around which the importance density must be centered, since the calculation of the gradients driving the search always yields zero.

In this work, we propose a new strategy for initializing the Kriging-based metamodels of the AKMCS and the AKIS, which relies on the assumption that a single point of failure in the DoE is sufficient for effectively starting the adaptive procedure for the refinement of the Kriging-based metamodel. This assumption is empirically verified with respect to two analytic case studies, in the next Section. Indeed, under this assumption, one may think of randomly sampling input points and evaluating the corresponding performance functions until a point of failure is encountered. However, this procedure would require a prohibitively large number of expensive performance function evaluations when the failure probability is very small. In fact, if  $P_f$  is of the order of  $10^{-q}$ , the number of samples required should be at least  $10^q$  to obtain, on average, one failure point.

Thus, we here propose a new method, called Latin Hypercube-based Search Algorithm (LHSA), aiming at identifying at least one input point belonging to the failure region by systematically proposing input points of increasing failure “likelihood” and evaluating the corresponding values of the performance function, until a failure (load shedding larger than zero) is found.

Operatively, the LHSA exploits a Latin Hypercube Sampling scheme for dividing the supports  $\mathcal{D}_{x_j}$ ,  $j = 1, \dots, n$ , of the cumulative density functions (cdf) describing the uncertainties of the input variables  $(x_1, \dots, x_n)$  in  $N$  iso-probable intervals. Fig. 1 shows how the range  $(0, 1]$  of a Gaussian cdf (chosen as an illustrative example) can be divided in  $N$  intervals of the same width, for  $N = 2, 4, 8, 16$ , giving rise to iso-probable intervals in the support  $\mathcal{D}_x$ , whose extremes are depicted by red crosses for the case  $N = 4$ . Under the assumption that the input variables are not correlated, the samples  $\{\mathbf{u}_j\}_i$ ,  $j = 1, \dots, n$ ,  $i = 1, \dots, N$ , are taken from a uniform distribution defined over each of the  $N$  equally sized intervals in the cdf range, for each of the  $n$  input variables.

Then, these values  $\{\mathbf{u}_j\}_i$  are randomly combined to form  $N$   $n$ -dimensional samples  $\mathbf{u}_i = \{u_1, \dots, u_n\}_i$ ,  $i = 1, \dots, N$ . Fig. 2 shows another illustrative example of a possible outcome of the procedure in the case of  $n=2$  input variables and  $N = 10$  iso-probable intervals. Up to this stage, the procedure is that of a standard Latin Hypercube sampling strategy [27]. Once the  $N$  samples  $\mathbf{u}_i$  are obtained, the LHSA evaluates the performance function  $\mathcal{G}(\mathbf{x})$  in correspondence of only the  $2n$  samples  $\mathbf{x}_l = \{x_1, \dots, x_n\}_l$ , with  $l = \operatorname{argmax}_{i=1, \dots, N} \{u_j\}_i$  or  $l = \operatorname{argmin}_{i=1, \dots, N} \{u_j\}_i$ , i.e., those corresponding to the vectors  $\mathbf{u}_i$  with one of their elements  $u_j$ ,  $j = 1, \dots, n$ , equal to either  $\max \{u_j\}_i$  or  $\min \{u_j\}_i$ , for  $j = 1, \dots, n$ , i.e., for example, the four points labeled by triangles in Fig. 2. By so doing, it performs the expensive evaluations of  $\mathcal{G}(\mathbf{x})$  only in the input regions of lower probability, i.e. those where the failure regions most likely lie. Fig. 1 shows these regions colored in grey for the illustrative example described above, when  $N = 16$ . Note that the  $2n$  samples  $\mathbf{x}_l = \{x_1, \dots, x_n\}_l$  are simply obtained by inverting the cdfs of the input variables in correspondence of the values  $\{u_j\}_i$ ,  $j = 1, \dots, n$ .

Since the aim is that of finding a failure point lying as close as possible to the limit state function, and not simply falling within the failure region, the LHSA starts its evaluations by dividing the supports  $\mathcal{D}_{x_j}$  in  $N = 2$  iso-probable intervals and proceeds doubling the value of  $N$  at each iteration, until it identifies a point of failure.

The LHSA is a semi-heuristic procedure, which does not guarantee the identification of a failure point and whose efficiency strongly depends on the shape of the failure domain in the original input space. In fact, in the particular case of a failure region completely surrounded by non-failure points (i.e., an island), then the iterative algorithm may miss it and the search would not come to an end. On the other hand, if the failure region were comprised in a very narrow multi-dimensional corner, many iterations (i.e., doublings of  $N$ ) might be necessary before a point in the failure region were randomly sampled. Another problem may arise in presence of multiple, disconnected failure regions of similar dimension: in this case, in fact, the LHSA would identify a point in only one of the regions and the subsequent failure probability estimation by a Kriging-based sampling scheme could turn out to be biased [22]. In principle, one may continue the search after the identification of the first failure point by the LHSA, but, in case other failures were identified, it would be hard to say whether they belong to the same failure region or not. Actually, this problem is shared by many other methods of literature (as, for example, the standard FORM or SORM [5–9]) and cannot be easily addressed, although some approaches have been proposed for adapting existing methods [22].

In our case, a stopping condition is introduced in the LHSA in order not to further divide the domain when unnecessary. The maximum number of intervals  $N$  is set to  $10^9$ , in order not to increase the computational effort without additional benefits. At this stage, if a failure point is not yet found, the reason lies on the way the independent uniform samples are paired and it is, thus, more efficient to restart the procedure from  $N = 2$ . Note that the maximum threshold can be changed, if a smaller probability has to be sampled.

The failure point identified by the LHSA can also be used as a “surrogate” of the MPFP for centering the importance densities of the AKIS, thus allowing, in principle, also the application of the AKIS to this kind of problems.

Finally, note that a zero-valued performance function  $\mathcal{G}(\mathbf{x})$  in correspondence of the non-failure points gives rise to another computational problem. In fact, regardless the number of examples available in the DoE and the accuracy of the corresponding Kriging-based metamodel, any approximation  $\mu_{\hat{\mathcal{G}}}(\mathbf{x})$  cannot be strictly equal to zero in the non-failure region, but it assumes both positive and negative (small) values. This, in turn, would lead to wrong classifications of the input samples and, consequently, to biased estimates of the failure probability. In order to overcome this issue, we artificially modify the output of the performance function by taking a properly chosen

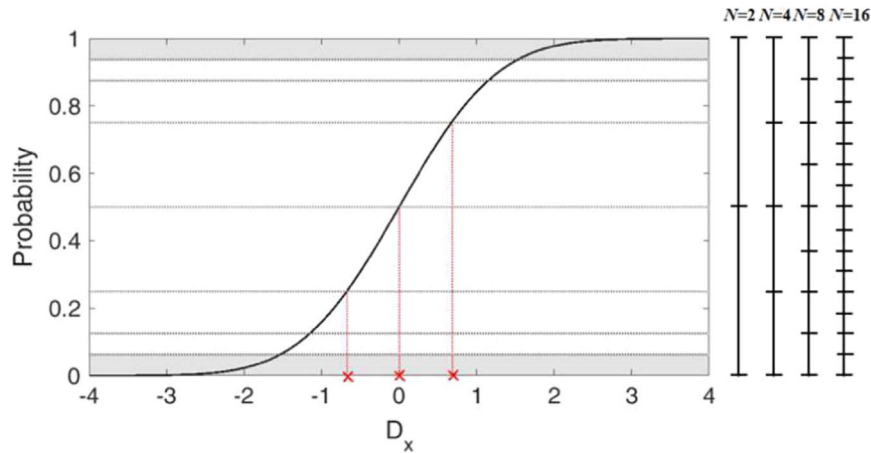


Fig. 1. Cumulative distribution function of a standard Gaussian random variable. The red crosses represent the extremes of the iso-probable intervals on the cdf support for  $N=16$ . The grey areas depict the iso-probable intervals in the cdf range where the samples are evaluated after four steps ( $N=16$ ) of the LHSA. (For interpretation of the references to color in this figure legend, the reader is referred to the web version of this article.)

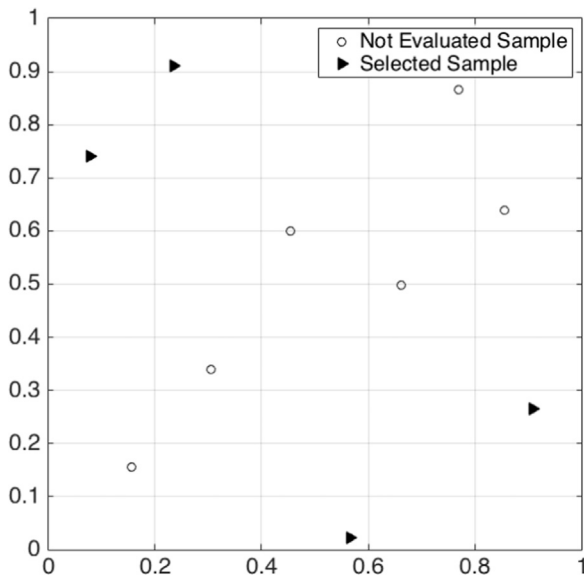


Fig. 2. Two-dimensional example of a selection process of the LHSA: the triangles indicate the points to be selected and evaluated.

constant, negative value  $T$ , instead of zero, each time the cascades do not lead to any load shedding. By so doing, the values reconstructed by the metamodel fluctuate around a negative, relatively large value, thus remaining negative, so that the estimate of the failure probability is not biased. On the other hand, we also introduce a discontinuity in the performance function to be approximated, which is in general more difficult to be captured by the metamodel, thus affecting the reconstructed position of the limit state. However, as demonstrated in the case studies of the next Section, the error introduced is largely compensated by the improvement due to the shift of the fluctuations and it is partially mitigated by the adaptive scheme of the algorithm.

Fig. 3 shows a flow chart which summarizes the operative procedure of the LHSA.

Note that both the AKMCS and AKIS algorithms are implemented by resorting to the DACE toolbox for the Kriging-based approximation of the performance function [35], where different kinds of regression and correlation models are available. As in [20–22], in this work ordinary Kriging is used along with an anisotropic exponential correlation model and linear regression.

### 3. Analytic case studies

In this section, we demonstrate the proposed algorithm on a one-dimensional case study and on a modified two-dimensional example often used in literature as a reference test case, both bearing some similarities with the problem addressed in this paper.

#### 3.1. One dimensional example

The performance function is defined as:

$$\mathcal{G}(x) = \begin{cases} 200 + 20 \cdot x & \text{if } x > k \\ 0 & \text{if } x \leq k \end{cases} \quad (10)$$

where  $x$  is the uncertain input, whose uncertainty is described by a standard Gaussian distribution, and  $k$  is a parametric threshold which can be used to set the failure probability  $P_f = P\{\mathcal{G}(x) > 0\}$  to any desired level. Note that (i)  $x=k$  is a discontinuity point for  $\mathcal{G}(x)$ , with an amplitude dependent on  $k$  and (ii) the performance function is always constant for  $x \leq k$ . The failure probability can be easily analytically computed, yielding  $P_f = 1 - \Phi(k)$ . The threshold is set to  $k = 2.6$ , so that the corresponding failure probability is  $P_f \cong 4.7 \cdot 10^{-3}$ .

According to the remarks at the end of the previous Section, we set  $\mathcal{G}(x) = -100$  for  $x \leq 2.6$ . Table 1 compares the results of the estimations performed with the proposed methods (LHSA+AKMCS, third row and LHSA+AKIS, fourth row) with those obtained by a crude Monte Carlo simulation (first row), where  $N_{calls}$  is the total number of performance function evaluations required. For completeness, we add the results obtained by coupling the LHSA technique with Importance Sampling, LHSA+IS (second row), which is similar to the classical FORM+IS approach, the difference lying in the fact that here the Gaussian importance density in the standard space is centered around the failure point found by the LHSA procedure, and not the MPPF. The comparison is carried out at approximately the same estimate error, i.e. the value of the corresponding coefficient of variation ( $\delta$ ). The values of Table 1 are obtained by averaging the results obtained by running the algorithms 30 times, for larger robustness. The LHSA requires only seven evaluations of  $\mathcal{G}(x)$  in order to identify one sample  $x > k$  of failure, whereas a pure random sampling would require approximately  $P_f^{-1} \cong 200$  runs. All the three methods presented offer significant improvements with respect to the crude Monte Carlo simulation in terms of the number of performance function evaluations required,  $N_{calls}$ . In this case study, the performances of the LHSA+AKMCS and LHSA+AKIS turn out to be almost the same, due to the effects of the adaptive stopping criterion adopted in the illustrated in Section 2, which ends the adaptation in both algorithms before significant

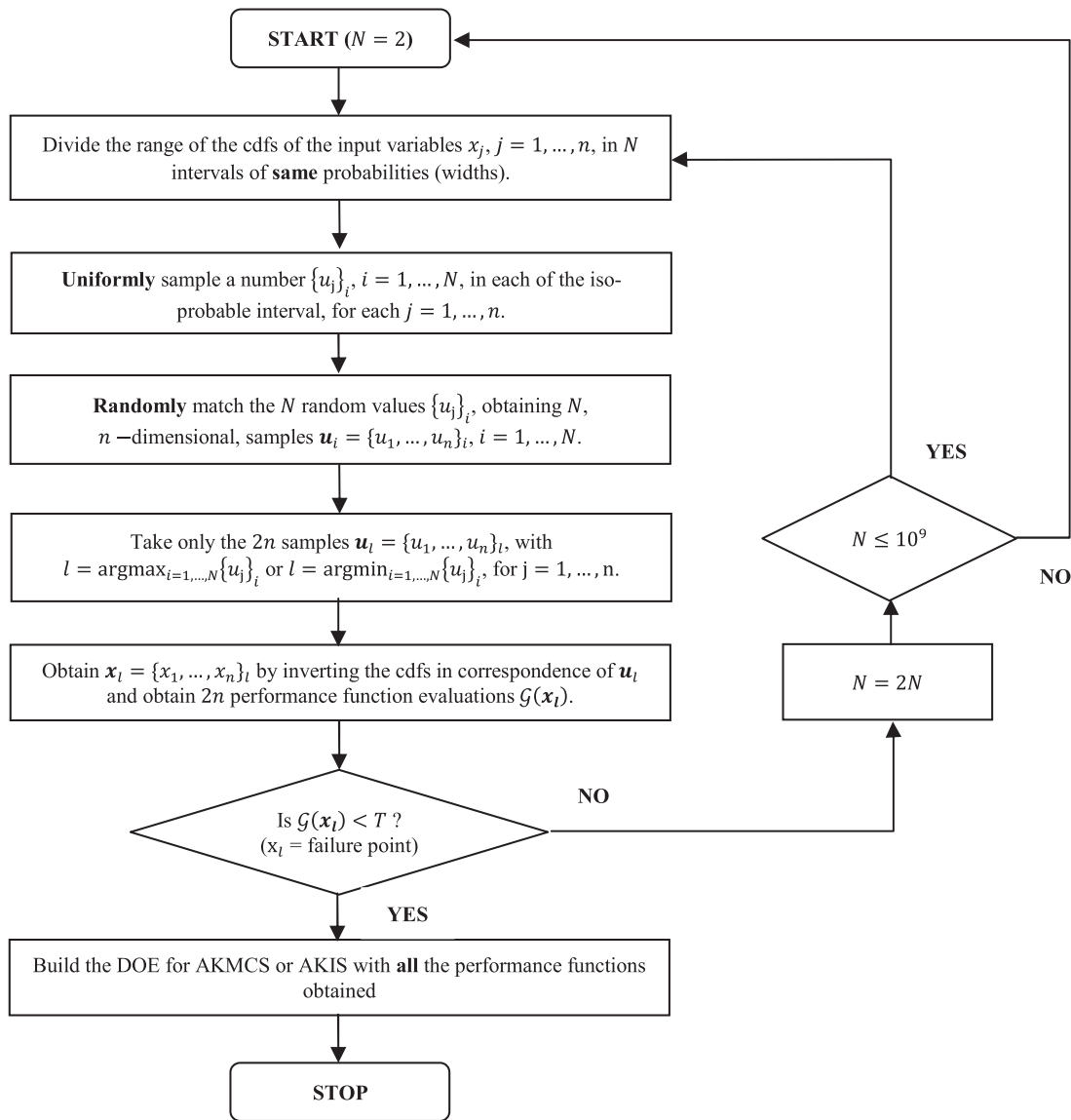


Fig. 3. Conceptual scheme of the LHSA.

Table 1  
Estimation performances for the one-dimensional example of Section 3.1, averaged over thirty repetitions of the simulations.

Method	$N_{calls}$	$P_f$	$\delta$ (%)
Crude MCS	$10^5$	$4.657 \cdot 10^{-3}$	4.626
LHSA+IS	7+1500	$4.705 \cdot 10^{-3}$	4.477
LHSA+AKMCS	7+203	$4.667 \cdot 10^{-3}$	4.618
LHSA+AKIS	7+203	$4.668 \cdot 10^{-3}$	4.617

differences in terms of number of performance function evaluations could emerge. The only difference lies in the number of evaluations of the Kriging-based metamodel required to approximately achieve the same coefficient of variation, i.e.  $N_{MC}=10^5$  and  $N_{IS}=1.5 \cdot 10^3$ : the consequences on the computational times in this case study are negligible, but in other applications involving lower failure probabilities and/or larger precision requirements, the difference may become significant [21]. Finally, as expected, both methods outperform the LHSA+IS, the difference being due to the use of a Kriging-based surrogate model in both the AKMCS and the AKIS for performing most of the performance function evaluations required.

In this example, we have thus shown that the AKMCS and AKIS

algorithms are capable of providing satisfactory results even when the initial DoE of the Kriging-based metamodel contains a single point of failure. However, it is worth verifying how the performances change if a different number of failure points in the initial DoE is chosen. In order to quickly find more failure points in the input space, we run again the LHSA to identify the first failure point and, then, we further sample new points from a normal distribution centered in the failure point and with standard deviation  $\sigma=1$ , until we obtain the required number of failure points. By so doing, the newly sampled points will more likely be of failure. Table 2 shows the results of the AKMCS run for different numbers of failure points in the initial DoE, averaged over 30 algorithm runs for achieving a larger robustness. Again, the comparison is carried out for approximately the same coefficient of variation  $\delta$ . A slight

Table 2  
Estimation performances for the one-dimensional example of Section 3.1, as a function of the number of failure points in the initial DoE.

# of failure points in the initial DoE	$N_{calls}$	$P_f$	$\delta$ (%)
1	7+203	$4.667 \cdot 10^{-3}$	4.618
5	14+202	$4.669 \cdot 10^{-3}$	4.617
10	23+190	$4.668 \cdot 10^{-3}$	4.618

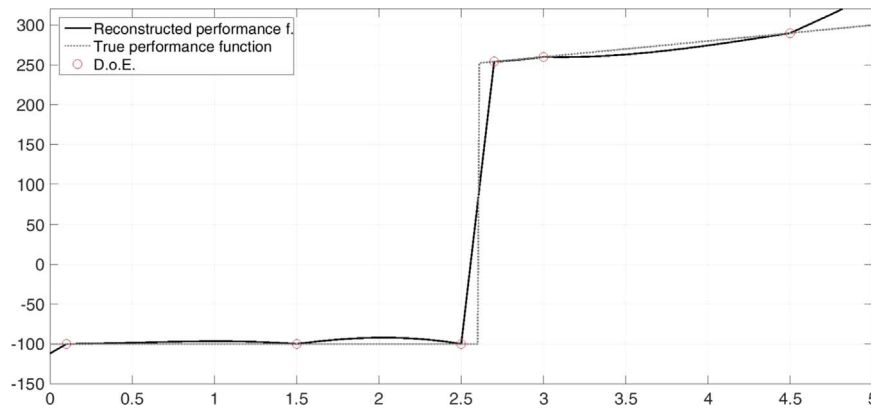


Fig. 4. Performance function reconstruction for the one-dimensional step function.

improvement in the number of performance function evaluations required by the AKMCS is observed only for the case of 10 failure points in the initial DoE. However, the total number of evaluations required, including the 24 needed to identify the 10 failure points, is not significantly better than that achieved in the case of a single failure point in the DoE. As noted also in [20], it is, thus, preferable to start with an initially poor DoE and let the active learning function of the Kriging-based sampling algorithm select the best new sample to be added to the DoE, since it is more informative than a random one sampled a-priori.

Finally, Fig. 4 shows the modified performance function  $\mathcal{G}(x)$  (solid line) and its corresponding approximation by the final Kriging-based metamodel obtained for the case with  $k = 2.6$  (bold), whose DoE contains six points (circles). It can be seen how the fluctuations of the reconstruction in correspondence of the non-failure points do not affect the classification, i.e. the values of  $\hat{I}_F(x)$ .

### 3.2. Modified two-dimensional case study of literature [21]

The performance function is [21]:

$$\mathcal{G}(x_1, x_2) = 0.5(x_1 - 2)^2 - 1.5(x_2 - 5)^3 - 3 \quad (11)$$

where  $x_1$  and  $x_2$  are two standard normal distributed random variables. Here, the performance function is modified as follows:

$$\mathcal{G}(x_1, x_2) = \begin{cases} 0.5(x_1 - 2)^2 - 1.5(x_2 - 5)^3 - 3 & \text{if } \mathcal{G}(x_1, x_2) > 0 \\ 0 & \text{if } \mathcal{G}(x_1, x_2) \leq 0 \end{cases} \quad (12)$$

in order to have a constant, zero output of the performance function in correspondence of the non-failure points. However, in view of the considerations made at the end of Section 2, we set  $\mathcal{G}(x_1, x_2) = q$ , where  $q$  is a constant, negative parameter, in order to avoid the misclassification issue. Indeed, the failure probability  $P_f = P\{G(x_1, x_2) > 0\}$  remains unchanged. We set  $q = -100$ . A crude MC simulation with  $N_{MC} = 10^7$  samples is run to obtain a reference value for  $P_f = P\{G(x_1, x_2) > 0\}$ , with a coefficient of variation  $\delta$  approximately equal to 6%.

Table 3 compares the results obtained with the crude MC simulation (first row) with those obtained by averaging 30 runs of the LHSA+IS (second row), LHSA+AKMCS (third row) and the LHSA+AKIS

Table 3

Estimation performances for the two-dimensional example of Section 3.2, averaged over thirty repetitions of the simulations.

Method	$N_{calls}$	$P_f$	$\delta$ (%)
Crude MCS	$10^7$	$2.915 \cdot 10^{-5}$	5.864
LHSA+IS	27+2500	$2.891 \cdot 10^{-5}$	5.639
LHSA+AKMCS	28+348	$2.882 \cdot 10^{-5}$	5.887
LHSA+AKIS	28+374	$2.712 \cdot 10^{-5}$	5.379

(fourth row) at approximately the same  $\delta$ . In the LHSA+IS, a population of  $N_{IS} = 2.5 \cdot 10^4$  input points is sampled from a joint standard Gaussian distribution centered around the failure point identified by the LHSA. The LHSA+AKMCS and the LHSA+AKIS significantly reduce the number of performance function evaluations,  $N_{calls}$ . However, as in the previous case study, they offer similar performances, due to the same reason explained before.

Note that the number of performance function evaluations achieved with the LHSA+AKIS is approximately one order of magnitude larger than that obtained in [21] on the similar case study. This was to be expected, however, since the importance density in the LHSA+AKIS is centered around a failure point close to the limit state, but different from the good approximation of the most probable failure point (MPFP) used in the AKIS of [21] and obtained with the FORM. As demonstrated in [15], even small differences from the actual position of the MPFP, may lead to poorer estimates of the failure probability, especially in larger dimensional input spaces. On the other hand, it would not be possible to use the AKIS of [21] for estimating the failure probability in the present case study, due to the constant value of the performance function in correspondence of non-failure points.

## 4. Cascading failures in a power transmission network

The test system is a version of the reference IEEE RTS 96 modified in [29,30] to account for additional power generation due to the presence of two wind farms (Wind Energy Conversion Systems) and to increase the vulnerability of the grid to cascading failures, for demonstrative purposes. The system operates with two different voltage levels, 138 and 230 kV, thus requiring the presence of transformer branches. The original grid model is composed by 24 nodes and 38 arcs, where each node represents a generating unit, a load point or a transmission/switch point. The specific topology and data regarding the generating capacity can be found in [28].

Here, we resort to a modified version of the stochastic framework developed in [29] for simulating the operations and the failures of an electric power transmission network subject to variable conditions, in order to quantify the contributions to unreliability due to the uncertainties of the total load required by the grid users, the ambient operating temperature and the wind speed acting on the grid lines and structures. As opposed to [29], where the dynamic evolution in time of the grid was simulated on an hourly basis and accounting also for the restoration of the network after any disruptive event, we here focus on the effects of the individual cascading failure events, possibly triggered by specific realizations of the operating conditions, without accounting for their timeline. The uncertain model inputs are treated as follows.

### 4.1. Power demand

In [29], the current power demand (load) is represented as a

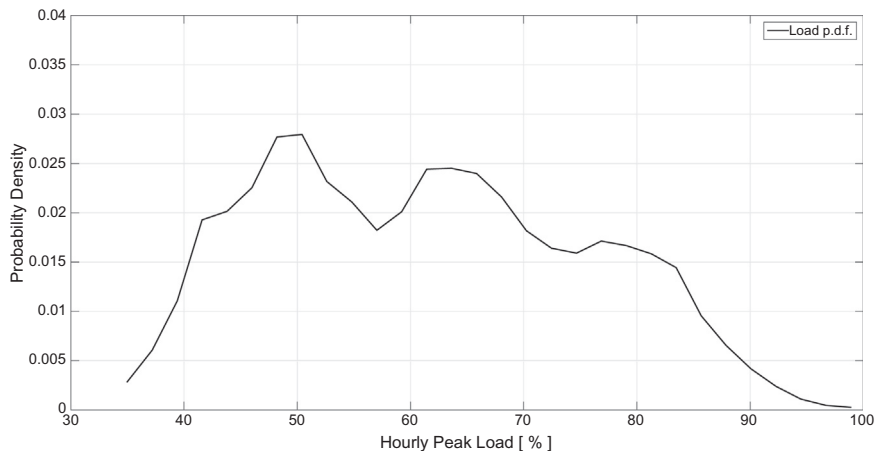


Fig. 5. Probability density function of the required load.

function of time on the basis of the hourly peak load taken from [28]:

$$\text{Current Load} = \text{Max load} * L_f * \text{Hourly Peak} (\%) \tag{13}$$

where  $\text{Max load} = 2850$  MW is the maximum total load requested by the system,  $L_f = 0.8$  is a load factor and the time varying hourly peak is expressed as the percentage of the maximum demand required. The available data account for customer power demand variations from day to night, weekdays and from season to season. In this work, since no temporal dependency is considered, a sample pdf of the current power demand is built on the basis of all the available hourly observations of the loads (Fig. 5). In other words, we assume that the Current Load is a realization of a stochastic, uncertain variable representing the power demand during a random hour of the year.

#### 4.2. Ambient temperature

In [29], the daily minimum and maximum values during one year are considered. A linear variation of the temperature values between the daily minimum and maximum values is assumed, with the minimum and maximum peaks registered at 5 a.m. and 4 p.m., respectively. Similarly to the case of the current load, since no temporal dependency is considered, a sample pdf of the ambient temperature (Fig. 6) is built on the basis of all the available hourly observations of the temperatures. Again, we assume that the ambient temperature is a realization of a stochastic, uncertain variable representing the temperature during a random hour in the year.

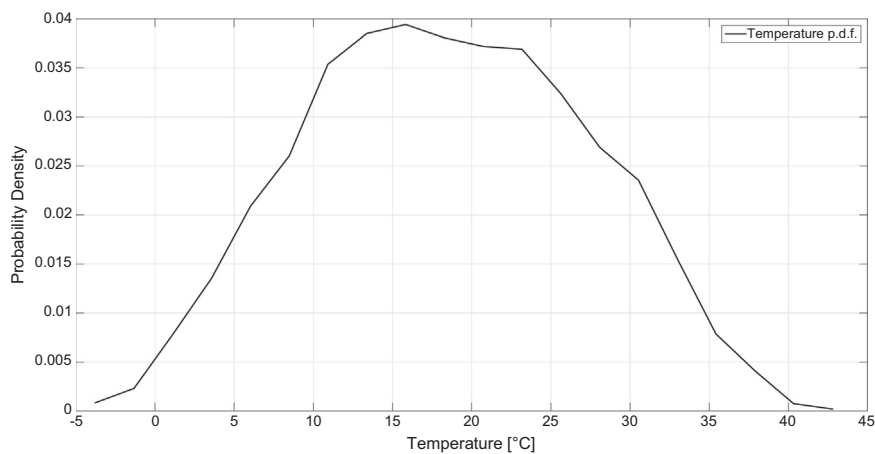


Fig. 6. Probability density function of the ambient temperature.

#### 4.3. Wind speed

In [29], to compute the wind speed curve, a set of hourly values has been retrieved from [36] and analyzed. Here, we assume that, for each day of the year, the wind speed is constant throughout the day and it is equal to the daily average value. Following [37], a Weibull distribution

$f(x, \alpha, \beta) = \frac{\alpha}{\beta^\alpha} x^{\alpha-1} e^{-\left(\frac{x}{\beta}\right)^\alpha}$ ,  $x \geq 0$ , is used to represent the wind speed uncertainty, with parameters estimated by maximum likelihood on the basis of the available hourly measurements [37], yielding a scale parameter  $\alpha = 1.15 \cdot 10^3$  and a shape parameter  $\beta = 28.3$  (Fig. 7). The wind speed is thus a realization of a stochastic, uncertain variable representing the wind speed during a random hour in a day.

#### 4.4. Wind power generation

The uncertainty in the wind speed propagates to the power output of wind turbine generators (WTGs), since the power output of a WTG directly depends on the wind regime as well as on the performance characteristics and the efficiency of the generator [38].

The power output from a WTG is determined using the functional relationships used in [39], linking the characteristics of a WTG and the wind speed field [40] (Fig. 8). The wind turbine generating unit can have four different operative states: a first standby phase, in which wind speed is lower than the cut-in wind speed ( $w_{cut-in} = 3$  m/s) and there is no power production; a second phase, in which power production increases with a cubic trend in the wind speed range between  $w_{cut-in}$  and the rated wind speed  $w_r$ , after which the power production is constant and equal to the WTG target power; finally,

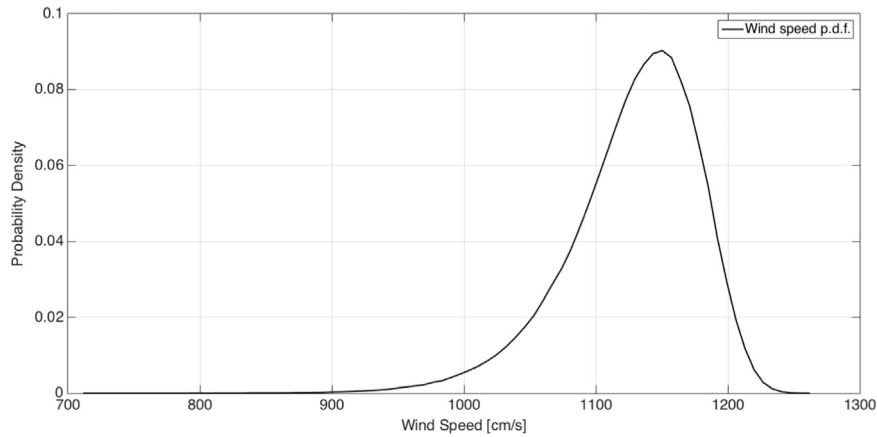


Fig. 7. Probability density function of the ambient temperature.

when the wind speed exceeds the maximum wind speed ( $w_{cut-off}=25$  m/s), the WTG is disconnected for protection purposes and the power production stops (cut-off phase). Hence, a wind turbine produces its maximum power, i.e. the rated power, within a certain interval that has its upper limit at the cut-out wind speed. Note that the WTG used in this work starts producing power when the wind speed equals the cut-in speed of 3 m/s, so that the larger fraction of wind power generation is produced during the nonlinear part of the output curve (Fig. 8).

As anticipated in the introduction, the unreliability of the transmission network is here measured by the frequency of occurrence of a total load shedding larger than zero at the end of the cascading events, possibly triggered by an initial line failure due to the occurrence of an undesired combination of the values of the three uncertain input variables, i.e. the total load ( $X_1$ ), the ambient temperature ( $X_2$ ) and the wind speed ( $X_3$ ).

Using the formalism of the Introduction, the output of the model, i.e., the final load shedding  $LS$ , can, then, be written as:

$$LS = \mathcal{G}(X_1, X_2, X_3) \quad (14)$$

The objective is that of estimating the failure probability  $P_f = P[LS > 0]$ , due to the uncertainties in the model inputs ( $X_1, X_2, X_3$ ). This failure probability can be taken as an indicator of the capability of the power grid to handle different scenarios, sustain hazards and, in case a failure occurs, efficiently re-dispatch power flows in order to avoid further propagation of the damages.

The power transmission grid is assumed to operate through steady-state conditions, also during the occurrence of major disturbances. Given an input scenario, the power generated and the power demanded (load) at each node of the grid, the full nonlinear alternate current (AC) power flow equations should be solved in order to determine the

operating conditions of the power grid, i.e., the powers flowing in each line, and to verify whether any line undergoes an overload, thus being automatically disconnected from the network by the protection systems and, possibly, triggering a cascading failure. However, the solution of the full non-linear power flow equations is computationally too demanding for the purposes of this work. Therefore, the power flow equations are linearized, thus obtaining the so-called direct current (DC) approximation [41,42], which are here solved by means of the MATLAB tool MATPOWER [43].

The approximate power flows in each line of the grid thus obtained represent the potential current configuration of the network, unless a line failure occurs due to a power flow exceeding its rated transmission capacity. Similarly to [29], the first line failure occurring, i.e. the one leading to the reconfiguration of the system and, possibly, to a cascade event, is identified on the basis of a failure model representing the line overheating dynamics [44]. Thus, the problem of heat conduction is analyzed for rods of small cross-section, in which an electric current of constant intensity flows. For simplicity, we assume that (i) each transmission line has constant physical properties, (ii) the temperature is constant at all points of its cross-section and (iii) the heat flux across the surface of the line is proportional to the temperature difference between the surface and the surrounding medium and is given by  $H(T_{rod} - T_0)$ , where  $T_{rod}$  is the temperature of the line,  $T_0$  is the temperature of the medium and  $H$  is the surface conductance. Since the heat source is equally distributed along the line, and assuming that fluctuations in the current flowing along the transmission lines propagate much faster than any heat flow transients, we can neglect the spatial variation in temperature along the line. Finally, in order to keep the heat equation linear, we neglect the heat exchanged by radiation with the surrounding medium, usually resulting in a cooling

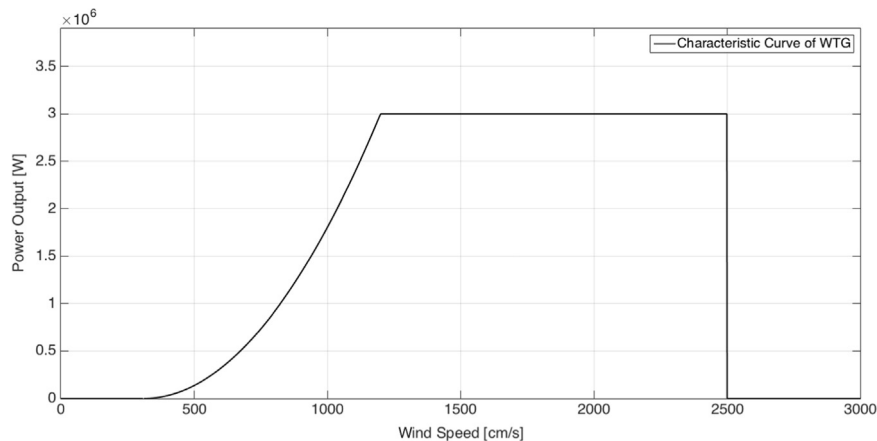


Fig. 8. Characteristic curve of the wind turbine generator.

term, especially when the wind is absent. Thus, a unique temperature is defined for each line, function of environmental conditions, current circulating and time. When the power flowing through the line changes up to exceeding its critical threshold, the rod will start heating, with the temperature increasing towards the equilibrium temperature corresponding to the new power flow. As the temperature grows, the line sag increases and, when the temperature overcomes its rating, line tripping automatically occurs. For further details on the heat model adopted, the interested reader may refer to [29,44].

Thus, in correspondence of a given set of values of the input variables ( $X_1, X_2, X_3$ ), the initial line failure (if any) is identified as the first one occurring among all the theoretically possible line disconnections due to overheating. As soon as the first line is disconnected, the DC power flow is calculated again and new lines may possibly overcome their rated capacities. In this case, the simulation of the cascade event proceeds in the same fashion, otherwise, it stops. During the propagating event, if unbalanced islands, i.e. disconnected portions of the grids, are formed, then the simple proportional re-dispatch strategy of [41] is adopted to achieve balance.

A crude MC simulation is performed to obtain the reference value for the failure probability  $P_f = P\{LS > 0\} \cong 4.80 \cdot 10^{-2}$ , with a coefficient of variation  $\hat{\delta}_{MC}$  lower than 5%. In order to do so, the cascading failures are possibly simulated in correspondence of  $N_{MC} = 10^4$  samples of the input variables ( $X_1, X_2, X_3$ ) and the corresponding final load shedding  $LS$  is recorded at the end of each simulation. In this case, the crude MC simulation could be performed in a reasonable computational time due to the relatively large value of the failure probability due to the simplifying modeling assumptions. For example, in reality more efficient and optimized re-dispatch strategies are adopted, which, in combination with other control tools available to the network operators, are such that cascading failures are almost always avoided. Note that, in order for the AKMCS and the AKIS to properly work, according to the considerations made in both the case studies of the previous Section with regards to the performances of the Kriging-based metamodel, we set  $LS = -200$  MW each time the actual final load shedding is equal to zero.

Table 4 compares the results obtained with the crude MC simulation (first row) with those obtained by averaging 30 runs of the LHSA+IS (second row), LHSA+AKMCS (third row) and the LHSA+AKIS (fourth row) at approximately the same  $\delta$ . LHSA is able to find a failure event with around 8 calls to the CM. In the LHSA+IS, a population of  $N_S = 10^3$  input points is sampled from a multivariate standard Gaussian distribution centered around the failure point identified by LHSA.

The LHSA+AKMCS and the LHSA+AKIS significantly reduce the number of performance function evaluations  $N_{calls}$ . Note that, in this case, the LHSA+AKIS shows performances slightly improved with respect to LHSA+AKMCS, suggesting that the coupling between the shape of the limit function and the natural input distribution is crucial to determine the convergence velocity of the method, especially if the AKIS process is not centered in the MPFP but in its approximation, identified by LHSA.

Fig. 9 shows the load shedding predicted by the final metamodel of the AKMCS algorithm as a function of the power load. It can be seen that the fluctuations due to the approximation errors do not significantly affect the classification of the input samples into failure or safe

points, which is also shown in the plane ( $X_1-X_3$ ) (current load – wind speed) in Fig. 10. Interestingly, the shape of the failure region in Fig. 10 also highlights that, given the input distributions adopted in this work, the current load demand is more important than the wind speed in determining whether an input scenario leads to load shedding larger than zero or not. Similar plots in the other planes, not shown here for brevity's sake, visually demonstrate that the ambient temperature is the least important. This was actually to be expected, since, besides the obvious significant importance of the load request, the wind speed has a double influence on the model, i.e. by affecting the heat equation in the line failure model and, most importantly, by modifying the power generated by the two wind farms, whereas the ambient temperature only affects the heat equation.

### 5. Conclusions

In this work, we have addressed the problem of estimating the probability of rare, failure events occurring in an electrical power transmission network subject to cascading failures triggered by uncertain boundary conditions. The peculiarity of the dynamic behavior of the system analyzed has required the adaptation of some efficient algorithms available in literature. More specifically, we have developed a new computational approach, called LHSA, for an alternative initialization of two algorithms of literature, i.e. the AKMCS and the AKIS, for the efficient estimation of the failure probability of a power transmission network operating under uncertain boundary conditions. The failure has been defined as the event that the grid undergoes an unsuccessfully controlled cascading failure leading to a final load shedding larger than zero. The new algorithm, based on a Latin Hypercube search of the space of the uncertain model inputs, has allowed a quick identification of at least one point of failure in a setting where the gradient of the performance function (i.e., the load shedding) with respect to the model inputs in the non-failure region, is always equal to zero. The identification of the point of failure has been shown to be sufficient for the adaptive construction of the Kriging-based metamodel used in both the AKMCS and the AKIS methods in two analytic case studies, properly constructed so as to bear similarities to where the combined LHSA+AKMCS and LHSA+AKIS algorithms offered satisfactory performances at a significantly lower number of performance function evaluations than the crude MC.

Then, the combined LHSA+AKMCS and LHSA+AKIS have been demonstrated to be capable of estimating the probability of a final load shedding larger than zero on a model of the reference IEEE14 power transmission network subject to cascading failures, possibly triggered by the uncertain operating conditions. The model has been purposely simplified in order to be able to achieve verifiable results in reasonable computational times, while maintaining those peculiar dynamic features which stimulated the investigation. Both combined methods provided satisfactory results at a relatively small number of evaluations of the network model.

The adaptability of the algorithm provided by the AK-module comes at the price of the unexpectedly low convergence speed observed in the simple, one-dimensional analytic example, which is due to the steep, hard to approximate shape of the performance function at the limit state. However, it should also be noted that the number of performance function evaluations required by the AK module remains of the same order of magnitude as the complexity and the dimensionality of the performance function increase.

It is worth reminding that both the AKMCS and the FORM+AKIS methods alone, i.e. without the proposed initialization module, cannot be used in this context, along with many other methods available in literature for the estimation of small failure probabilities, even potentially more efficient. For example, the FORM/SORM methods (and those exploiting their results, such as FORM+IS) are based on the approximation of the derivatives of the performance function, which, in our case, are always equal to zero in the safe region, so that, without

**Table 4**  
Estimation performances for the power transmission grid model, averaged over thirty repetitions of the simulations.

Method	$N_{calls}$	$P_f$	$\delta$ (%)
Crude MCS	$10^4$	$4.80 \cdot 10^{-2}$	4.41
LHSA+IS	$9 \cdot 10^3$	$4.77 \cdot 10^{-2}$	3.67
LHSA+AKMCS	8+297	$4.80 \cdot 10^{-2}$	4.45
LHSA+AKIS	8+207	$4.69 \cdot 10^{-2}$	3.56

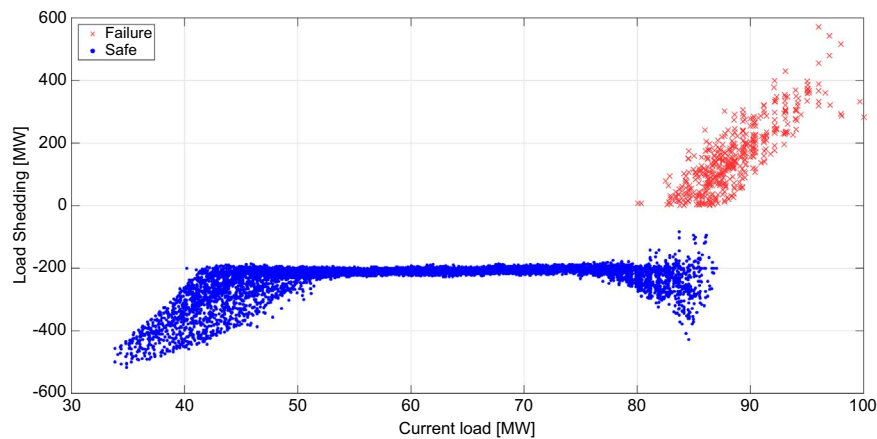


**Fig. 9.** Predicted load shed as a function of the required load. The red crosses represent the samples classified as failures by the Kriging-based metamodel, while the blue dots are the non-failure points. (For interpretation of the references to color in this figure legend, the reader is referred to the web version of this article.)

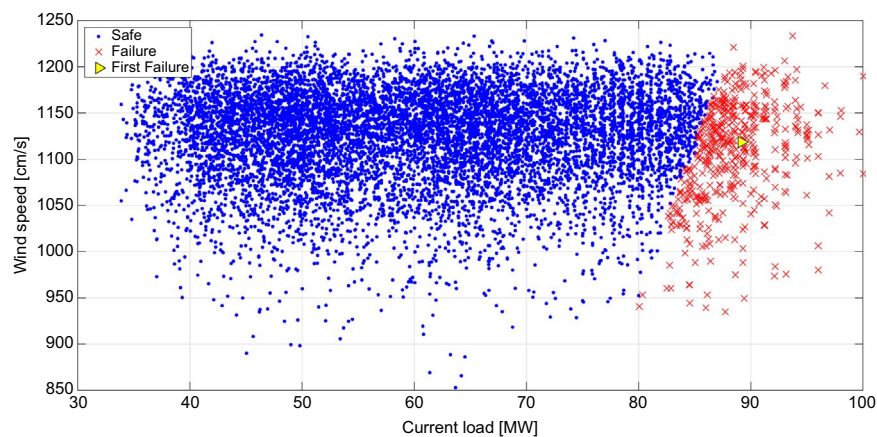


**Fig. 10.** Two-dimensional projection (wind speed vs. current load) of the limit state. The red crosses represent the samples classified as failure by the Kriging-based metamodel, while the blue dots are the non-failure points. The triangle is the failure point identified by the LHSA. (For interpretation of the references to color in this figure legend, the reader is referred to the web version of this article.)

any prior knowledge, no information can be gained on the position of the failure region. Subset simulation also would not work, due to the impossibility of setting intermediate failure levels in the failure regions, nor line sampling, for which it would be hard to efficiently identify the important direction with the initializing approaches proposed so far. In this last regard, possible alternative approaches not using the AK-module (thus not incurring in the risk of low efficiencies when approximating step-wise discontinuous functions) may consider using the LHSA i) to support the identification of the most important direction and then apply a line sampling module or ii) to find the initial failure point from which to start a MCMC for the direct estimation of the failure probability. Both approaches are currently under investigation.

Finally, note that the proposed approach can be more generally applied to engineered systems where constant outputs characterize the range of “nominal” operating conditions, whereas drifts, offsets or anomalous behaviors are observed in correspondence of rare, undesired operating conditions.

## References

- [1] Liscouski B, Elliot W. U.S.–Canada power system outage task force. *System* 2004;40:238.
- [2] Maas GA, Bial M, Fijalkowski J. Final report—system disturbance on 4 November 2006. Union for the Coordination of Transmission of Electricity; 2007. [Online]. Available: (<http://scholar.google.com/scholar?hl=en&btnG=Search&q=intitle:Final+Report+System+Disturbance+on+4+November+2006#1>)
- [3] U.S. Department of Energy. The smart grid. Communication, 99; 48; 2010
- [4] Final report of the investigation committee on the 28 September 2003 Blackout in Italy. Union for the Co-ordination of transmission of Electricity (UCTE); 2004. [Online]. Available: (<http://www.ucte.org>).
- [5] Sudret B. Meta-models for structural reliability and uncertainty quantification. In: Phoon K, Beer M, Quek S, Pang S, editors. In: Proceedings of the 5th Asian-Pacific symposium on structural reliability and its applications. Singapore; 2012. pp. 53–76
- [6] Melchers R. Radial importance sampling for structural reliability. *J Eng Mech* 1990;116(1):189–203.
- [7] Lemaire M. *Structural reliability*. Great Britain, United States: ISTE Wiley; 2009.
- [8] Ditlevsen O, Madsen HO. *Structural reliability methods*. Chichester, West Sussex, England: John Wiley & Sons; 1996.
- [9] Der Kiureghian A, Lin HZ, Hwang SJ. Second-order reliability approximations. *J Eng Mech* 1987;113(8):1208–25.
- [10] Schueller GI, Stix R. A critical appraisal of methods to determine failure probabilities. *Struct Saf* 1987;4(4):293–309.
- [11] Bucher CG. Adaptive sampling—an iterative fast Monte Carlo procedure. *Struct Saf* 1988;5(2):119–26.
- [12] Ang GL, Ang AHS, Tang WH. Optimal importance sampling density estimator. *J Eng Mech* 1992;118(6):1146–63.
- [13] Au SK, Beck JL. A new adaptive importance sampling scheme for reliability calculations. *Struct Saf* 1999;21:135–58.
- [14] Schueller GI, Pradlwarter HJ, Pandey MD. Methods for reliability assessment of nonlinear systems under stochastic dynamic loading – a review. In: Proceedings of EURO-DYN’93. Balkema; 1993. pp. 751–759
- [15] Katafygiotis LS, Zuev KM. Geometric insight into the challenges of solving high-dimensional reliability problems. *Probab Eng Mech* 2008;23(2–3):208–18.
- [16] Au SK, Beck JL. Estimation of small failure probabilities in high dimensions by subset simulation. *Probab Eng Mech* 2001;16(4):263–77.
- [17] Cadini F, Avram D, Pedroni N, Zio E. Subset simulation of a reliability model for radioactive waste repository performance assessment. *Reliab Eng Syst Saf* 2012;100:75–83.
- [18] Dubourg V, Sudret B, Deheeger F. Metamodel-based importance sampling for structural reliability analysis. *Probab Eng Mech* 2013;33:47–57.
- [19] Koutsourelakis PS, Schueller GI, Pradlwarter HJ. Reliability of structures in high dimensions, part I: algorithms and applications. *Probab Eng Mech* 2004;19:409–17.

- [20] Echard B, Gayton N, Lemaire M. AK-MCS: an active learning reliability method combining Kriging and Monte Carlo simulation. *Struct Saf* 2011;33(2):145–54.
- [21] Echard B, Gayton N, Lemaire M, Relun N. A combined Importance Sampling and Kriging reliability method for small failure probabilities with time-demanding numerical models. *Reliab Eng Syst Saf* 2013;111:232–40.
- [22] Cadini F, Santos F, Zio E. An improved adaptive Kriging-based importance technique for sampling multiple failure regions of low probability. *Reliab Eng Syst Saf* 2014;131:109–17.
- [23] Cadini F, Gioletta A, Zio E. Improved metamodel-based importance sampling for the performance assessment of radioactive waste repositories. *Reliab Eng Syst Saf* 2015;134:188–97.
- [24] Cadini F, Gioletta A. Bayesian Monte Carlo-based algorithm for the estimation of small failure probabilities of systems affected by uncertainties. *Reliab Eng Syst Saf* 2016;153:15–27.
- [25] Cadini F, Gioletta A, Zio E. Estimation of passive systems functional failure probabilities by the modified meta-IS algorithm. *Prog Nucl Energy* 2015;81:134–40.
- [26] Cadini F, Santos F, Zio E. Passive systems failure probability estimation by the meta-AK-IS<sup>2</sup> algorithm. *Nucl Eng Des* 2014;277:203–11.
- [27] Stein M. Large sample properties of simulations using Latin hypercube sampling. *Technometrics* 1987;29(2):143–51.
- [28] Grigg C, Wong P, Albrecht P, Allan R, Bhavaraju M, Billinton R, et al. The IEEE reliability test system-1996. A report prepared by the reliability test system task force of the application of probability methods subcommittee. *IEEE Trans Power Syst* 1999;14(3):1010–20.
- [29] Sansavini G, Piccinelli R, Golea LR, Zio E. A stochastic framework for uncertainty analysis in electric power transmission systems with wind generation. *Renew Energy* 2014;64:71–81.
- [30] Billinton R, Gao Y, Karki R. Composite system adequacy assessment incorporating large scale wind energy conversion systems, considering wind speed correlation. *IEEE Trans Power Syst* 2009;24(3).
- [31] Rasmussen CE, Williams CKI. *Gaussian processes for machine learning*. Cambridge, MA: MIT Press; 2006.
- [32] Muller WG. *Collecting spatial data. Optimum design of experiments for random fields*. Physica-Verlag, Heidelberg, Germany; 2001
- [33] Cox DD, John S. SDO: a statistical method for global optimization. In: Alexandrov MN, Hussaini MY, editors. *Multidisciplinary design optimization: state-of-the-art*. Philadelphia: Siam; 1997. p. 315–29.
- [34] Liu P-L, Der Kiureghian A. Multivariate distribution models with prescribed marginals and covariance. *Probab Eng Mech* 1986;1(2):105–12.
- [35] Lophaven SN, Nielsen HB, Sondergaard J. DACE, a Matlab Kriging toolbox, version 2.0. Technical Report IMM-TR-2002-12. Technical University of Denmark; 2002. [Online] Available: (<http://www2.imm.dtu.dk/~hbn/dace/S>)
- [36] Mohamed FA, Koivo HN. System modelling and online optimal management of microgrid using mesh adaptive direct search. *Int J Electr Power Energy Syst* 2010;32(5):398–407.
- [37] Johnson GK. *Wind energy systems*. Electron edition; 2006
- [38] Thiringer T, Linders J. Control by variable rotor speed of a fixed-pitch wind turbine operating in a wide speed range. *IEEE Trans Energy Convers* 1993;8(3):520–6.
- [39] Jin T, Tian Z. Uncertainty analysis for wind energy production with dynamic power curves. In: *IEEE Proceedings of the 11th international conference on probabilistic methods applied to power systems*. San Marcos, TX, USA, 14e17 June 2010
- [40] P. Giorsetto K.F. Utsurogi Development of a new procedure for reliability modeling of wind turbine generators. *IEEE Transactions on Power Apparatus and Systems* (Volume: PAS-102, Issue: 1, Jan. 1983), p. 134-143
- [41] Dobson I, Carreras BA, Lynch VE, Newman DE. An initial model for complex dynamics in electric power system blackouts. In: *Proceedings of the 34th annual Hawaii international conference on system sciences*; 2001. doi: <http://dx.doi.org/10.1109/HICSS.2001.926274>
- [42] Allen J, Wood BFW. *Power generation operation and control*. J.W. & S. Inc. editors. Second edition, Wiley-Interscience; 1996
- [43] Zimmerman RD, Murillo Sánchez CE, Thomas RJ. *MATPOWER: “steady-state operations, planning, and analysis tools for power systems research and education*. *IEEE Trans on Power Syst* 2011;26(1):12–9.
- [44] Carslaw HS, Jaeger JC. *Conduction of heat in solids*, 2nd ed.. Oxford: Clarendon Press; 1959.